

Simulating the dynamics of flexible wood pulp fibres in suspension

John M. Stockie
Department of Mathematics and Statistics
University of New Brunswick
Fredericton, NB, Canada, E3B 5A3
stockie@unb.ca

Abstract

We investigate the dynamics of a flexible, elastic fibre, suspended in a fluid and subjected to a 3D shear flow. Simulations are performed using the “Immersed Boundary Method,” and are distinguished by their ability to capture the hydrodynamic interaction between the fluid and fibre, as well as the detailed structure of the individual fibres. Suspensions of flexible fibres are encountered in many industrial problems, although we focus in this work on the application to wood pulp fibre suspensions.

1 Introduction

The study of suspensions of long, thin particles is of great importance in a wide range of applications, including wood pulp processing, polymer composites, and formation of fibre-reinforced materials such as plastics, concrete, etc. Owing to the tendency of long, slender particles to orient themselves in the direction of the flow, suspensions of such particles exhibit fluid properties that depend on fibre orientation. Concentrated suspensions are well-known to exhibit a non-linear fluid stress-strain relationship which leads to flow behaviour very different from that seen in simple fluids or dilute suspensions. However, before being able to formulate a model for concentrated suspensions which accurately captures fluid-fibre and fibre-fibre interactions, it is essential to have an intimate understanding of the dynamics of fibres in dilute suspensions. Direct simulations of a small number of fibres can be used to compute distributions of quantities such as orientation angle and intrinsic viscosity [9] which may then be exploited to build better rheological models for concentrated suspensions.

To this end, a significant body of recent work has appeared in the literature on direct numerical simulations of fibres in suspension. Most simulations of a large number of particles ignore the flexing of individual fibres and instead treat the suspended particles as one-dimensional rigid bod-

ies which are characterised solely by position and orientation (for example, [4, 16]). However, it is well-known that suspensions of flexible fibres behave very differently than rigid ones [6], and so simulations that take into account fibre flexibility are essential.

Most previous simulations of flexible particles are based on mechanical models in which a suspended fibre is divided into a sequence of massless, solid bodies that are linked by joints allowing bending, twisting, and possibly also stretching motions (see [11, 14, 15]). In all of the aforementioned works, the fibres are subjected to a *given* shear flow which exerts a predetermined hydrodynamic force the fibre, and hence the fibres have no influence on the dynamics of the surrounding fluid. Previous work by the present author [13] has shown that including the two-way hydrodynamic interaction between fibre and fluid can capture phenomena (namely, skewed orientation angle distributions) which are observed in experiments but are not captured by these other simulations. Furthermore, fibre models based on solid, rigid bodies are incapable of capturing important characteristics of particles such as wood cells that have a very well-defined internal structure (described in Section 3).

In the present work, we present simulations of a flexible fibre using the *immersed boundary method* [8]. In the immersed boundary framework, which we outline in Section 2, flexible 3D structures are built by interweaving one-dimensional elastic elements to form a surface that resists bending and stretching. This is a natural construction for wood cells, which have an underlying structure consisting of layers of cellulose fibrils, described in detail in Section 3. We focus on the application to wood pulp suspensions subjected to a planar shear flow, which occur in several stages of the paper-making process. Our immersed boundary model for a wood cell is described in Section 2, and numerical simulations using the *Immersed Boundary General Software Package* or IBGSP [3] are presented in Section 4. The IBGSP is a distributed-memory implementation of the code developed in [7, 8] for simulating blood flow in the heart on the Cray series of shared-memory su-

percomputers.

The originality of this work stems from several considerations, one of the most important being that these are the first simulations of pulp fibres which take into account the actual physical structure of a wood cell; namely, its non-circular cross-section, hollow centre, and cellulose fibril construction. Furthermore, these are the first direct numerical simulations to include the influence of a deforming fibre on the surrounding fluid, hence capturing the two-way interaction between fluid and fibre. Finally, this is one of the few non-biological applications of the immersed boundary method which further demonstrates the efficacy of the method to a wide range of problems in fluid-structure interaction.

2 The Immersed Boundary Method

In this section, we provide a brief description of the immersed boundary method (or “IB Method”) and the underlying model equations. Full details of the model and its implementation are available in the literature, for example [8]. The precursor of the present work was a two-dimensional model for wood pulp fibres developed in [13].

2.1 The Model Equations

The IB Method is distinguished by its ability to simulate the motion of complex, deforming, elastic structures simply and efficiently. Other methods for handling fluid-structure interaction tend to be significantly more complex and computationally intensive, due to their use of explicit front-tracking or moving grids to ensure that the computational coordinates coincide with the position of the immersed structure.

In the IB model, a deformable, elastic boundary or surface is immersed within an incompressible fluid that lies on both sides of the surface. The fluid motion is governed by the incompressible Navier-Stokes equations,

$$\rho \frac{\partial \mathbf{u}}{\partial t} = -\rho \mathbf{u} \cdot \nabla \mathbf{u} + \mu \Delta \mathbf{u} - \nabla p + \mathbf{F}, \quad (1)$$

$$\nabla \cdot \mathbf{u} = 0, \quad (2)$$

where $\mathbf{u}(\mathbf{x}, t)$ and $p(\mathbf{x}, t)$ are the fluid velocity and pressure at any time t and position $\mathbf{x} = (x, y, z)$ in space.

We next describe the specification of the external force, $\mathbf{F}(\mathbf{x}, t)$, which is the force exerted by the immersed boundary on the neighbouring fluid particles. In the IB model, an immersed boundary is constructed out of an interwoven network of 1D, massless elements or “immersed fibres” (not to be confused with the pulp fibres under consideration here, which have a 3D structure) that consist of points connected to each other by “springs” or “links.” A single linear element, Γ_k , can be described by position $\mathbf{X}_k(s, t)$, where s

is a parameter which can be taken to be the arclength along the fibre in an unstressed configuration. Then, the elastic force exerted by the k^{th} immersed fibre can be written as

$$\mathbf{F}_k(\mathbf{x}, t) = \int_{\Gamma_k} \mathbf{f}_k(s, t) \cdot \delta(\mathbf{x} - \mathbf{X}_k(s, t)) ds, \quad (3)$$

where $\mathbf{f}_k(s, t)$ is the force density and $\delta(\mathbf{x}) = \delta(x) \cdot \delta(y) \cdot \delta(z)$ is a three-dimensional Dirac delta function. A typical spring-like restoring force would be given by a force density of the form $\mathbf{f}_k(s, t) = \partial^2 \mathbf{X}_k / \partial s^2$. The collective influence of a set of n_f immersed fibres, Γ_k , for $k = 1, 2, \dots, n_f$ is then given by the sum $\mathbf{F} = \sum_{k=1}^{n_f} \mathbf{F}_k$.

The fluid and immersed boundary motions are then coupled together by the requirement that the boundary must move at the velocity of neighbouring fluid particles, otherwise known as the “no-slip condition,”

$$\frac{\partial \mathbf{X}_k}{\partial t} = \mathbf{u}(\mathbf{X}_k(s, t), t) \quad (4)$$

$$= \int_{\Omega} \mathbf{u}(\mathbf{x}, t) \cdot \delta(\mathbf{x} - \mathbf{X}_k(s, t)) d\mathbf{x}, \quad (5)$$

where the integral in the second (equivalent) form is taken over the entire fluid domain, Ω .

2.2 The Numerical Method

The fluid–fibre system represented by equations (1)–(5) represents a coupled system of nonlinear, integro-differential equations that must be solved for \mathbf{u} , p , and \mathbf{X} . The fundamental idea in the IB Method is that the fluid equations are discretised on a fixed, rectangular, grid, having constant grid spacing $h = \Delta x = \Delta y = \Delta z$. The immersed boundary, on the other hand, is described by another set of points which are allowed to move relative to the underlying fluid grid. This avoids having perform any complicated front tracking or grid remeshing near an interior boundary, which is a significant disadvantage of many other methods for fluid-structure interaction problems. The efficiency of the IB Method derives from the following two considerations:

- the immersed boundary influences the fluid solely through the forcing term \mathbf{F} in equation (1), and hence we can employ fast, efficient fluid solvers for rectangular grids. In particular, for problems with periodic boundary conditions, an explicit pressure projection scheme based on a Fast Fourier Transform is often an excellent choice.
- the interaction between fluid and fibre through equations (3) and (5) is computed using convolutions with Dirac delta functions, which are handled in the IB

method by replacing $\delta(x)$ with a discrete approximation such as $d_h(x) = \frac{1}{4h} (1 + \cos(\frac{\pi x}{2h}))$ for $|x| < 2h$. Hence, all integrals are replaced by quadratures involving points lying in a region of width $4h$ in each coordinate direction, which can be computed very efficiently.

Using the spatial discretisation outlined above, the equations are then integrated in time using the following explicit approach:

1. At each immersed boundary point, the force densities, \mathbf{f} , are calculated from the current boundary positions, \mathbf{X} . These forces are then distributed onto fluid grid points using equation (3).
2. At each fluid grid point, the velocity and pressure are updated (under the influence of the force \mathbf{F}) by integrating the Navier-Stokes equations using a split-step projection method.
3. Finally, the new fluid velocities are used to compute updated values of the immersed boundary positions \mathbf{X} using equation (5).

Full details of the numerical method can be found in [8] or [13].

2.3 Immersed Boundary General Software Package (IBGSP)

The IBGSP [3] is a Fortran-77 implementation of the IB method based on a code written by Peskin and McQueen [7, 8] to compute the flow of blood within a beating heart on shared-memory machines such as the Cray C-90. The IBGSP has totally revamped the data structures in this very specialised code in order to handle a much more general class of fluid-structure interaction problems. More importantly, the code has been redesigned for implementation on both serial machines and distributed-memory machines such as the SGI Origin. At the present time, the code runs in serial mode only, but an MPI-based implementation for SGI machines will be available in the near future. The IBGSP is also supplemented by a high-quality, 3D visualisation package which allows easy, interactive, exploration of the computed results.

The portion of the algorithm devoted to the fluid solver (Step 2.) is particularly easy to implement efficiently on parallel machines since it can take advantage of the native FFT's that are optimised for a given architecture. Likewise, the computation of the fibre forces is also easily parallelizable. However, the force and velocity interpolation stages (in Steps 1. and 3.) involve interactions between fluid and boundary points which by far make up the majority of the cost in a given computation. Because the boundary points move relative to the underlying fluid grid, they have no logical connection or ordering in relation to the fluid points,

and so these interpolation steps are extremely challenging to implement efficiently in parallel. Some of the issues related to implementation for shared memory machines are detailed in [7].

3 Immersed Boundary Model of a Pulp Fibre

Wood pulp consists of a suspension of hollow, fibres ranging from 0.1 to 0.3 *cm* in length, and having an aspect ratio between 30 and 100. The fibres are tapered to points at each end, and the cross-sections are not circular (as is true with many man-made fibres) but rather rectangular with rounded corners. The walls of the wood cell are

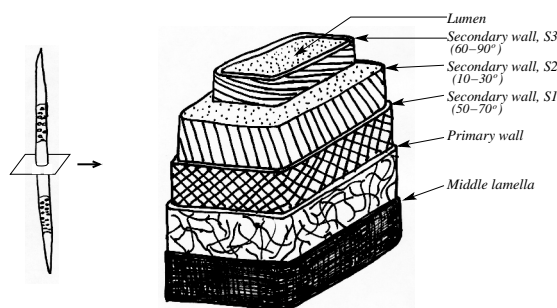


Figure 1. Left: A mature softwood fibre. Right: A close-up, cut-away view showing the cellulose fibril layers (adapted from [2, Fig. 2-4] and [10, Fig. 115]), which also indicates the range of winding angles for each layer. The secondary walls form the basis of our immersed boundary model for the wood cell.

composed of interwoven cellulose *fibrils*, which lend the wall its strength and flexibility. In the cut-away view of a wood cell in Figure 1, it is also evident that the cell wall consists of several distinct layers, each characterised by a different orientation of the cellulose fibrils.

Consequently, the immersed boundary method seems to be a natural framework in which to simulate the motion of these cells, wherein the force-bearing points lie along curves, \mathbf{X}_k , which have a close correspondence to cellulose fibrils. We focus in particular on the three layers in the cell wall which have a well-defined fibril orientation, namely the S1, S2 and S3 secondary layers, and construct

an immersed boundary model that is depicted in Figure 2. The S1 fibrils, in Figure 2(a), are wound helically about the circumference in both directions, with a *winding angle* of $\phi \approx 50 - 70^\circ$, measured relative to the axis of the wood cell. The S2 fibrils, in Figure 2(b), have a winding angle of $\phi \approx 10 - 30^\circ$, which we approximate as purely axial fibrils. Finally, the S3 layer, in Figure 2(c), are much more steeply inclined at an angle of $\phi \approx 60 - 90^\circ$, which we replace by a sequence of circumferential rings inclined at $\phi = 0$.

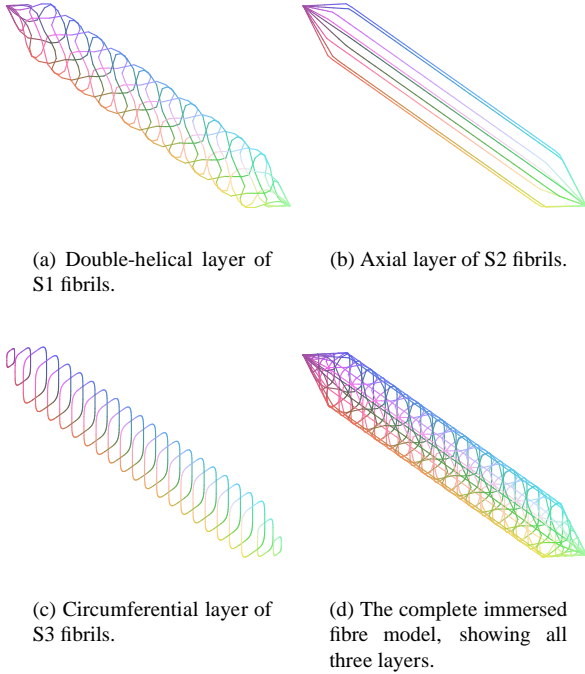


Figure 2. The layered construction of our 3D wood fibre model, showing the immersed boundary analogue of the cellulose fibrils.

All immersed boundary points are connected to their successive neighbours by spring-like links that resist stretching and compression. While it is possible to introduce bending-resistant forces into our immersed boundary model, this is not necessary because the interwoven structure of immersed boundaries naturally gives rise to a bending rigidity. Furthermore, we can ensure that the model wood cell length remains approximately constant (like real cells) provided we take the elastic stiffness to be large enough. When our model cell is placed into a fluid flow, the fibre is able to bend and deform under the action of fluid stresses. Note that fluid lies both inside and outside of the wood cell; as a result of the incompressibility condition, and the no-slip condition on the cell walls, the internal pressure

of the fluid maintains the general shape of the cell.

4 Numerical Simulations

We now present immersed boundary simulations of a single wood cell having length 0.4 cm , immersed within a periodic fluid box with dimensions 1 cm on a side. Consequently, these results correspond to a regular, periodic array of fibres which form an idealised version of a dilute suspension. The cell is constructed out of 14 helical (S1) fibrils, 13 axial (S2) fibrils, and 32 circumferential (S3) fibrils. The fluid domain is divided into a 32^3 grid, with grid spacing $h = \frac{1}{32}$. The immersed boundary points located on each fibril are chosen so that the separation between these points is at most $\frac{h}{2}$ (this is a requirement that minimises the interpolation error from using discrete delta functions, and hence avoids any leakage of fluid). Consequently, a total of approximately 2100 immersed boundary points are required to describe the configuration of the wood cell, and 32768 points for the fluid. A typical simulation requires slightly over 60 minutes of clock time on an Silicon Graphics Onyx2 machine (with two 195 MHz IP27 processors).

The fluid and fibre motions are driven by a planar shear flow which is generated by including point forces on fluid grid points that lie on the planes $x = 0.20$ and $x = 0.80$. The wood cell is placed at the centre of the domain, equally-spaced between the two shear planes, and the fluid and fibre are started from rest.

In the following three numerical simulations, we consider wood cells with different flexibility and initial configurations and show that our computed trajectories reproduce some of the qualitative behaviours of real pulp fibres. Experiments on flexible fibres subjected to a shear flow ([1] for example) show that the fibres exhibit very well-defined orbital dynamics that differ based on the fibre flexibility and symmetry of the initial conditions.

Rigid pulp fibre: We first consider a short, thick, wood cell (with aspect ratio 10) which essentially rotates as a rigid body. From the time sequence shown in Figure 3, it is clear that the shear flow causes the cell to rotate approximately in the x, z -plane, as is expected from experiments on rigid fibres subjected to shear. We have retained the periodic images of the solution in the z -direction in order that the upstream flow can be visualised. The marker particles included in these plots indicate that the fluid flow in the neighbourhood of the wood cell is clearly not a simple shear flow. Other methods which ignore the influence of the deforming pulp fibre on the local fluid dynamics will miss this effect.

Flexible fibre undergoing an S-turn: Next, we increase the aspect ratio to 30, which makes the fibre much more

flexible, and take a fibre that is initially straight and symmetric. The resulting dynamics pictured in Figure 4 are known as an “S–turn,” and match qualitatively with orbits observed in experiments [1]. Similar dynamics are also reproduced in other numerical simulations using symmetric initial conditions [12, 6], but these other methods are unable to capture the fine details of fibre deformations which are evident in our results.

Flexible fibre undergoing a snake turn: The final case we consider is a non-symmetric situation, in which the fibre is initially given a slight bend at one end (see the index $N = 0$ plots in Figure 5). All other parameters are identical to that from the previous example. In contrast with earlier results, the subsequent fibre orbit in this case is non-symmetric, although the period of rotation is similar. This is in fact the type of orbit most commonly observed in experiments on flexible fibres since the level of initial symmetry required to obtain an S–turn is almost never seen real wood fibres.

5 Conclusions

In this paper, we presented simulations of a single flexible wood pulp fibre suspended in a planar shear flow, using the immersed boundary method. We have attempted to capture the cellulose fibril microstructure of a wood cell as accurately as possible using interwoven, elastic, “immersed fibres” which resist stretching and compression. The simulations are able to capture the hydrodynamic interaction between the fluid and the fibre and so capture the fibre deformation and fluid dynamics in unprecedented detail. Our numerical results demonstrate that the method is capable of capturing the full range of fibre orbital behaviours observed in experiments. This work also has the potential to have major impact in the development of improved rheological models for concentrated particle suspensions.

Our comparisons with other experimental and numerical results are so far only qualitative, and so a great deal of work is still required in order to validate the model and numerical results. First of all, numerical experiments must be performed to determine the actual flexural strength of wood cells which we construct out of interwoven immersed fibres. Once flexibility can be measured, then we can make more quantitative comparisons to experiments and carefully investigate how the orbital type, period, and orientation angle distribution depend on various physical parameters.

Acknowledgments

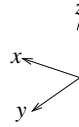
I would like to express my sincere appreciation to Nathaniel Cowenn (Tulane University) for his help with the

Immersed Boundary General Software Package. I would also like to thank Charles Peskin and David McQueen for many helpful discussions, and for providing access to the excellent computing facilities while I was visiting the Courant Institute.

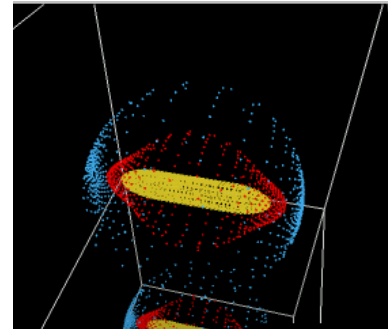
References

- [1] A. P. Arlov, O. L. Forgacs, and S. G. Mason. Particle motions in sheared suspensions IV. General behaviour of wood pulp fibres. *Svensk Papperstidn.*, 61(3):61–67, 1958.
- [2] C. J. Biermann. *Handbook of Pulping and Papermaking*. Academic Press, San Diego, second edition, 1996.
- [3] N. S. Cowen, D. M. McQueen, and C. S. Peskin. Immersed Boundary General Software Package (IBGSP), release 1.0.0. Available on request from peskin@cims.nyu.edu, 1999.
- [4] X. Fan, N. Phan-Thien, and R. Zheng. A direct simulation of fibre suspensions. *J. Non-Newton. Fluid Mech.*, 74:113–135, 1998.
- [5] K. Gustavsson, J. Ooppelstrup, and J. Eiken. Consolidation of concentrated suspensions – shear and irreversible floc structure rearrangement. *Comput. Visual. Sci.*, 4:61–66, 2001.
- [6] C. G. Joung, N. Phan-Thien, and X. J. Fan. Direct simulation of flexible fibers. *J. Non-Newton. Fluid Mech.*, 99:1–36, 2001.
- [7] D. M. McQueen and C. S. Peskin. Shared-memory parallel vector implementation of the immersed boundary method for the computation of blood flow in the beating mammalian heart. *J. Supercomput.*, 11:213–236, 1997.
- [8] C. S. Peskin and D. M. McQueen. A three-dimensional computational model for blood flow in the heart. I. Immersed elastic fibers in a viscous incompressible fluid. *J. Comput. Phys.*, 81:372–405, 1989.
- [9] C. J. S. Petrie. The rheology of fibre suspensions. *J. Non-Newton. Fluid Mech.*, 87:369–402, 1999.
- [10] P. A. Roelofsen. *The Plant Cell-Wall*. Gebrüder Borntraeger, Berlin, 1959.
- [11] R. F. Ross and D. J. Klingenberg. Dynamic simulation of flexible fibers composed of linked rigid bodies. *J. Chem. Phys.*, 106(7):2949–2960, Feb. 1997.

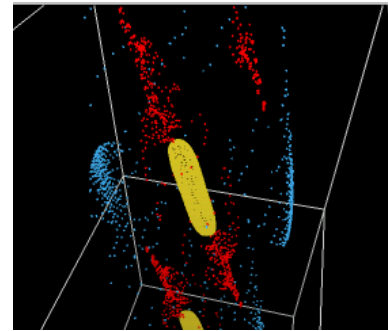
- [12] P. Skjetne, R. F. Ross, and D. J. Klingenberg. Simulation of single fiber dynamics. *J. Chem. Phys.*, 107(6):2108–2121, 1997.
- [13] J. M. Stockie and S. I. Green. Simulating the motion of pulp fibres using the immersed boundary method. *J. Comput. Phys.*, 147(1):147–165, 1998.
- [14] G. Wherrett, I. Gartshore, M. Salcudean, and J. Olson. A numerical model of fibre motion in shear. In *Proceedings of the 1997 ASME Fluids Engineering Division Summer Meeting*, Vancouver, Canada, June 22–26, 1997.
- [15] S. Yamamoto and T. Matsuoka. A method for dynamic simulation of rigid and flexible fibers in a flow field. *J. Chem. Phys.*, 98(1):644–650, Jan. 1993.
- [16] Y. Yamane, Y. Kaneda, and M. Doi. Numerical simulation of semi-dilute suspensions of rodlike particles in shear flow. *J. Non-Newton. Fluid Mech.*, 54, 405–421 1994.



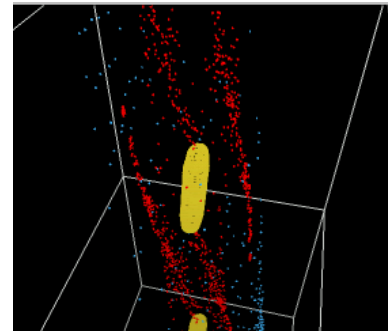
N = 0



N = 12



N = 24



N = 36

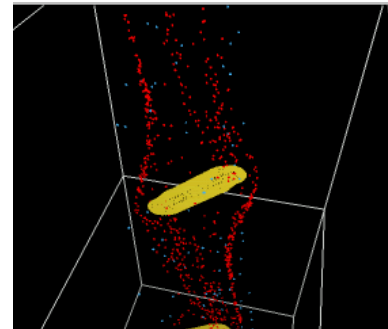


Figure 3. A rigid wood cell immersed within a shear flow, including marker particles (blue and red) that help visualise the flow around the cell.

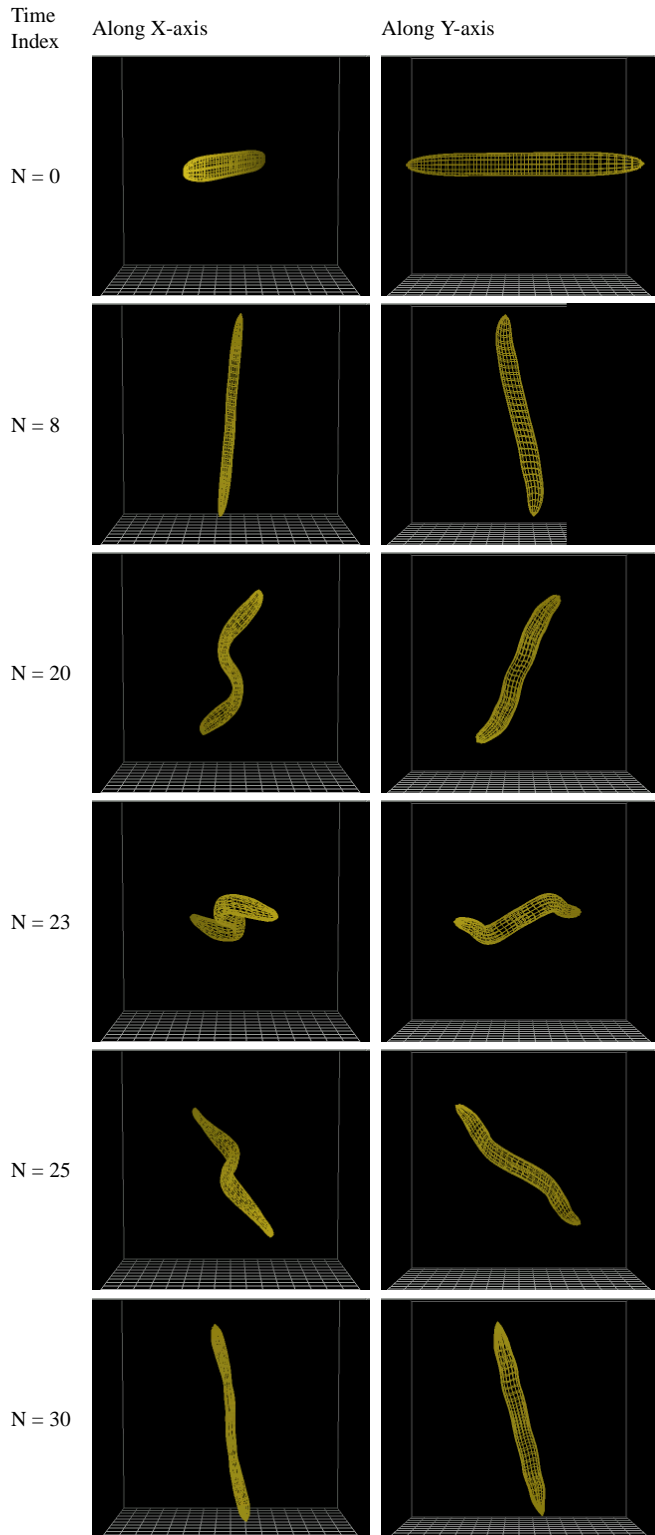


Figure 4. An initially straight fibre executes a symmetric “S-turn orbit.”

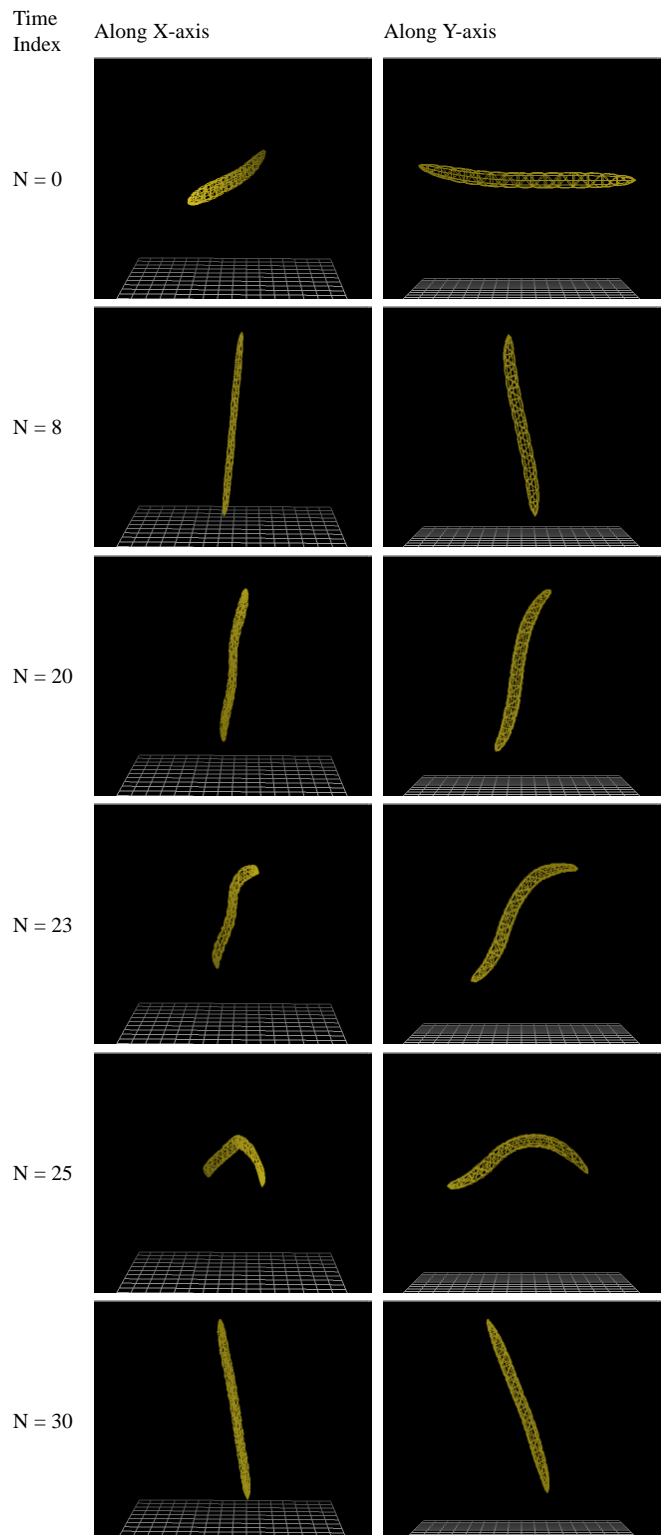


Figure 5. A fibre with asymmetric initial conditions executes a “snake orbit.”